Propagation Characteristics of the Magnetostatic Surface Wave in the YBCO-YIG Film-Layered Structure

Makoto Tsutsumi, *Member, IEEE,* Takeshi Fukusako, *Student Member, IEEE,* and Shigeo Yoshida

***Abstract*— Propagation characteristics of the magnetostatic surface wave (MSSW) in a $YBa_2Cu_3O_{7-x}$ (YBCO)-yttrium iron garnet (YIG) multilayered structure are investigated. Effects of the superconductor on the MSSW are discussed with regard to the dispersion characteristics of both the phase and attenuation constants as a function of the air gap between YIG and YBCO, taking into consideration the magnetic line-width of the YIG film. It was found that the nonreciprocity of MSSW is enhanced significantly by the superconductivity and depends on the magnetic line-width of the YIG film. To examine the effect of a YBCO on the MSSW propagation, experiments are carried out using a commercially available YIG film. Magnetic losses at low temperature are briefly discussed with experimentally observed nonreciprocity.**

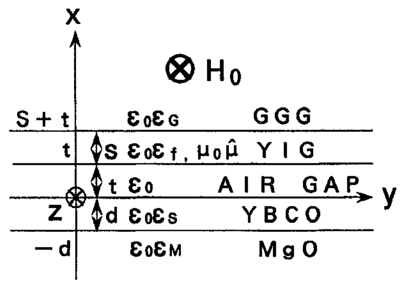

Fig. 1. Magnetostatic surface waveguide composed from a YBCO-YIG layered structure.

I. Introduction

SINCE THE discovery of superconducting materials, applications of high-temperature superconductors to microwave and millimeter wave devices and circuits have been intensely investigated [1]. Many papers on theory and experimental characteristics of microstrip lines, filters, and resonators with high and low temperature superconducting materials have been published. Most papers emphasized the microwave superconducting devices with dielectric materials.

Little effort has been devoted to the studies on nonreciprocal superconducting circuits and devices, such as circulators, isolators and phase shifters using polycrystalline ferrites [2], [3]. Although the surface impedance of a superconductor in a dc magnetic field is increased [4], the ability of the superconductor to significantly reduce propagation loss has been preserved.

Yttrium iron garnet (YIG) film epitaxially grown on a gadolinium gallium garnet (GGG) substrate has been widely used for magnetostatic wave (MSW) devices [5]. YIG films are preferred over the polycrystalline ferrite since line-width ΔH is narrower in epitaxial films [6][7].

In this paper, propagation characteristics of the magnetostatic surface wave (MSSW) in a YBCO ($YBa_2Cu_3O_{7-x}$)-YIG film-layered structure is analyzed with emphasis on the attenuation and phase constants, taking into consideration the air gap between YBCO and YIG, and also the magnetic line-width ΔH of YIG. Results are compared with experiments on nonreciprocal behavior using a commercially available YIG film prepared on GGG by the epitaxial technique, and the YBCO prepared on a MgO substrate using the laser ablation technique.

Manuscript received June 29, 1995; revised April 19, 1996.

The authors are with the Faculty of Engineering and Design, Kyoto Institute of Technology, Kyoto-shi, 606, Japan.

Publisher Item Identifier S 0018-9480(96)05653-0.

II. Dispersion and Attenuation

The waveguide geometry consists of the YBCO-YIG multilayered structure. A cross-view of the waveguide structure is shown in Fig. 1. The high-temperature superconductor YBCO of thickness d deposited on the semi-infinite MgO substrate is separated from a YIG film of thickness s on the semi-infinite GGG substrate by an air gap t. The MgO, GGG, and YIG are characterized by dielectric constants $\varepsilon_M, \varepsilon_G$, and ε_f. An external static magnetic field H_0 is applied in the plane of the YIG film. The MSSW propagates parallel to the plane of the YIG film in the y direction.

In the two-fluid model, the superconductor medium is defined by the relative dielectric constant [8]

$$\varepsilon_s(\omega) = \left(1 - \frac{\omega_s^2}{\omega^2} - \frac{\omega_n^2\tau_n^2}{\omega^2\tau_n^2+1}\right) - j\frac{\omega_n^2\tau_n}{\omega(\omega^2\tau_n^2+1)} \qquad (1)$$

where $\omega_s^2 = e^2n_s/m\varepsilon_0, \omega_n^2 = e^2n_n/m\varepsilon_0$ are the plasma frequencies of superparticles and normal particles. n_s and n_n are the number densities of electron pairs and normal particles, respectively, and the temperature dependence of n_s and n_n can be closely approximated by the Gorter-Casimir expressions

$$\frac{n_s}{n} = 1 - \left(\frac{T}{T_c}\right)^4, \quad \frac{n_n}{n} = \left(\frac{T}{T_c}\right)^4, \quad n = n_s + n_n \qquad (2)$$

where T_c is the critical temperature of the superconductor.

Assuming $\omega^2\tau_n^2 \ll 1$, (1) can be rewritten as

$$\varepsilon_s = \left(1 - \frac{1}{\omega^2\mu_0\lambda_L^2\varepsilon_0}\right) - j\frac{\sigma}{\omega\varepsilon_0} \tag{3}$$

where $\lambda_L^2 = \lambda_0^2/[1-(T/T_c)^4]$, λ_0 is the field penetration depth at temperature $T = 0$ K, and $\sigma = \sigma_n(T/T_c)^4$ [8]. The relative permeability tensor of the YIG film is given in the x, y, z representation of Fig. 1

$$\hat{\mu} = \begin{bmatrix} \mu & -j\kappa & 0 \\ +j\kappa & \mu & 0 \\ 0 & 0 & 1 \end{bmatrix}$$
$$\mu = 1 + \frac{\omega_h\omega_m}{\omega_h^2 - \omega^2}, \quad \kappa = \frac{\omega\omega_m}{\omega_h^2 - \omega^2}$$
$$\omega_h = \gamma\left(H_0 + j\frac{\Delta H}{2}\right), \quad \omega_m = \gamma 4\pi M_0 \tag{4}$$

where M_0 is the magnetic saturation, γ is a gyromagnetic ratio and the magnetic line-width ΔH which indicates the magnetic loss tangent is taken into account [6][7]. The coordinate system which is used for the analysis is illustrated in Fig. 1. The z direction is chosen along the dc magnetic field H_0.

The wave equation in the superconductor is obtained from Maxwell's equation

$$\nabla \times \boldsymbol{H} = j\omega\varepsilon_0\varepsilon_s\boldsymbol{E}, \quad \nabla \times \boldsymbol{E} = -j\omega\mu_0\boldsymbol{H} \tag{5}$$

with the relative dielectric constant of (3), and in the YIG film

$$\nabla \times \boldsymbol{H} = j\omega\varepsilon_0\varepsilon_f\boldsymbol{E}, \quad \nabla \times \boldsymbol{E} = -j\omega\mu_0\hat{\mu}\cdot\boldsymbol{H} \tag{6}$$

with the permeability tensor of (4).

Since the rf fields are independent of $z, \partial/\partial z = 0$, the TE mode (E_z, H_x, H_y) decouples to the TM mode (H_z, E_x, E_y) in Maxwell's equation [(5) and (6)]. The TE mode is important because the MSSW propagates in the TE mode even if the magnetostatic approximation in (6) is assumed [6]. For the wave traveling in the y direction, electric field E_z will have a dependence of $\exp(\mp j\beta y)$. The following expressions for E_z obtained from (5) in the superconductor

$$E_z = (A_1 \sinh k_{x1}x + A_2 \cosh k_{x1}x)e^{\mp j\beta y} \quad -d < x \le 0 \tag{7}$$

where

$$k_{x1} = \sqrt{\beta^2 - \omega^2\varepsilon_0\varepsilon_s\mu_0}$$

and obtained from (6) in the YIG film

$$E_z = \{B_1 \cosh k_{x2}(x-t) + B_2 \sinh k_{x2}(x-t)\}e^{\mp j\beta y} \quad t < x < t+s \tag{8}$$

where

$$k_{x2} = \sqrt{\beta^2 - \omega^2\varepsilon_0\varepsilon_f\mu_0\mu_{ef}} \quad \text{and} \quad \mu_{ef} = (\mu^2 - \kappa^2)/\mu.$$

The E_z component in the semi-infinite MgO substrate is

$$E_z = Ce^{\gamma_1(x+d)}e^{\mp j\beta y} \quad x \le -d \tag{9}$$

where $\gamma_1 = \sqrt{\beta^2 - \omega^2\varepsilon_0\varepsilon_M\mu_0}$.

The E_z component in the semi-infinite GGG substrate is given by

$$E_z = De^{-\gamma_2(x-s-t)}e^{\mp j\beta y} \quad t + s \le x \tag{10}$$

where

$$\gamma_2 = \sqrt{\beta^2 - \omega^2\varepsilon_0\varepsilon_G\mu_0}$$

and E_z in the air gap is

$$E_z = (E_1 \sinh k_{x3}x + E_2 \cosh k_{x3}x)e^{\mp j\beta y} \quad 0 < x \le t \tag{11}$$

where

$$k_{x3} = \sqrt{\beta^2 - \omega^2\varepsilon_0\mu_0}.$$

By requiring the tangential components of the electromagnetic field to be continuous at the boundaries, and eliminating unknown coefficients $A_1, A_2, B_1, B_2, C, D, E_1$, and E_2 of (7)–(11), the following transcendental equation is obtained as shown in (12) at the bottom of the page. This follows, where

$$F = \frac{k_{x3}(\gamma_1 \tanh k_{x1}d + k_{x1})}{k_{x1}(\gamma_1 + k_{x1}\tanh k_{x1}d)}$$
$$G = \kappa\beta(\kappa\beta \mp \mu\mu_{ef}\gamma_2) - \mu^2k_{x2}^2$$
$$H = \mu\mu_{ef}k_{x3}(\pm\kappa\beta - \mu\mu_{ef}\gamma_2).$$

The dispersion relation of (12) is estimated numerically. The material parameters used in the calculation are as follows:

$$\lambda_0 = 2200\ \text{Å}, \quad \sigma_n = 6.56 \times 10^6\ \text{s/m}, \quad T_c = 86\ \text{K},$$
$$4\pi M_0 = 1730\ \text{Gauss}, \quad \text{and} \quad H_0 = 130\ \text{Oe}.$$

The frequency dependence of the phase constant β for $T/T_c = 0.9$ and $\Delta H = 0$ is illustrated in Fig. 2. For the purpose of this calculation, the superconductor is either in contact with the YIG ($t = 0$) or removed ($t = \infty$). Fig. 2 shows that the bandwidth of the dispersion curve for $t = 0$ is different for β^+ ($+y$ direction, 1.4 GHz–2.8 GHz) and β^- ($-y$ direction, 1.4 GHz–5.2 GHz) due to the metallization, showing nonreciprocity [6] and that there is a transition point from positive to negative group velocity for $t = 20\ \mu$m and 40

$$\tanh k_{x2}s = \frac{\mu^2\mu_{ef}k_{x2}[(\gamma_2 + Fk_{x3})\sinh k_{x3}t + (F\gamma_2 + k_{x3})\cosh k_{x3}t]}{(G + FH)\sinh k_{x3}t + (FG + H)\cosh k_{x3}t} \tag{12}$$

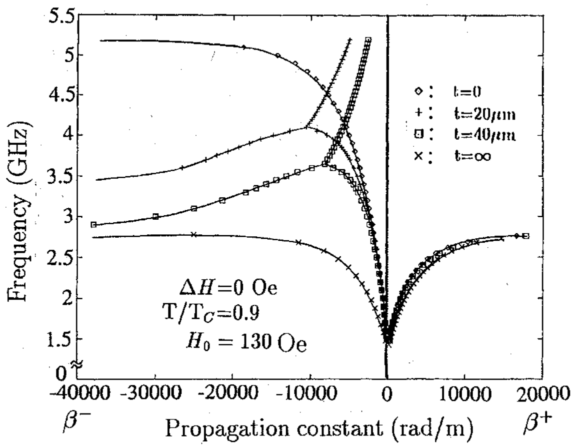

Fig. 2. Phase constant of the dispersion curve for different air gaps.

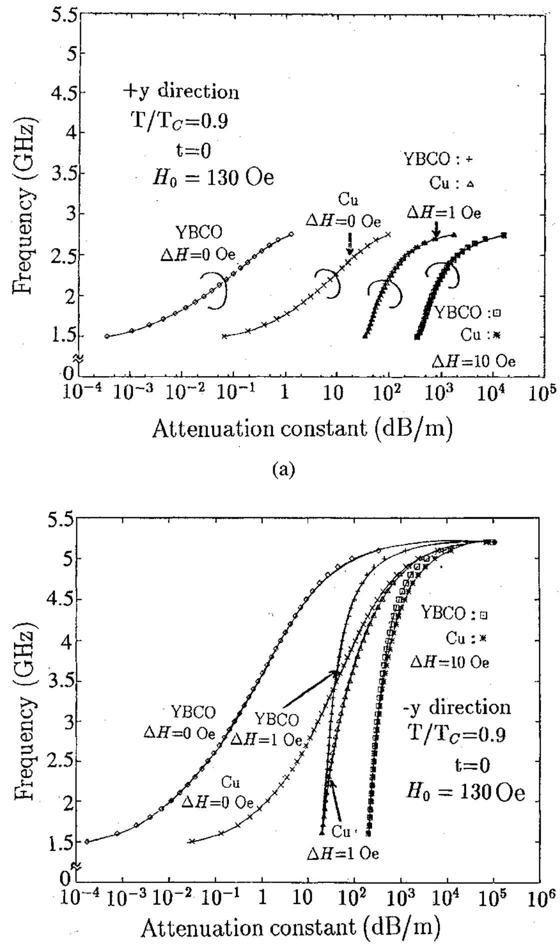

(a)

(b)

Fig. 3. Attenuation constant of the dispersion curve for a zero air gap.

μm, and it has a peak. This means nonreciprocity decreases as the air gap increases.

With the superconductor removed ($t = \infty$), the graph reverts to the typical dispersion curve of a magnetostatic surface wave, showing the same frequency range in the dispersion curve from 1.4 GHz to 2.8 GHz for the two propagation directions $\pm y$ [6]. It was found through calculations that the phase constant was not significantly affected by the ΔH and the critical temperature T/T_c. Fig. 3 shows the attenuation constant for various values of ΔH, a zero air gap and $T/T_c = 0.9$ which have the same frequency range of the phase constant of Fig. 2. The attenuation constant for the copper case is also shown in the figure for comparison to the characteristic of superconductor where σ of copper is assumed to be $\sigma = 4.5 \times 10^8$ s/m at 77 K.

It can be seen that the propagation loss is reduced significantly due to the superconductor effect compared to copper loading for the case of $\Delta H = 0$, and a marked difference in propagation loss characteristics for the two propagation directions $\pm y$ for $\Delta H = 1$ Oe, and they do not have the same frequency bandwidth for the $\pm y$ directions. However, the attenuation constant increases with increasing ΔH, and when ΔH exceeds 10 Oe, the attenuation is the same as for copper in the $\pm y$ directions. Thus, the large ΔH value of YIG film (more than 10 Oe) will degrade the loss reduction effect of the superconductor in the magnetostatic waveguide. It increases the total loss so that the improvement in the conduction loss brought by the YBCO is negligible. Fig. 4 shows the attenuation constant as a function of frequency for an air gap of 20 μm. It can be seen from the figures that loss is reduced due to the superconductor in the nonreciprocal frequency region above 2.5 GHz in a bias field of 130 Oe.

III. Experimental Results

To examine the effect of the YBCO on the MSSW propagation, experiments were undertaken by using a commercially available YIG film. The waveguide structure is shown in Fig. 5.

A high-temperature superconducting film of YBCO was deposited using the laser ablation technique on a 1 mm thick MgO substrate. The YBCO film has a thickness of 6000 Å, critical temperature of $T_c = 86$ K, and dimensions of $20 \times 15\,\text{mm}^2$. The half wavelength microstrip line filter [9] with such YBCO shows excellent microwave superconducting properties. The 100 μm thick YIG film was epitaxially grown on a 400 μm thickness, $5 \times 17\,\text{mm}^2$ GGG substrate. The magnetic line-width ΔH of the film is 1 Oe at X band. The YBCO was attached mechanically to the YIG film through a mica spacer as shown in Fig. 5. The fine-wire input output transducers (diameter of 100 μm) are located on the YIG film edges with 16 mm of separation. A pair of Helmholtz coils of 300 turns each is provided to apply a dc bias field to the YIG film in the transverse direction of MSSW propagation. The magnetic field intensity was 200 Oe for one ampere electric current at the center of the coil. The waveguide, together with the Helmholtz coils, was immersed in liquid nitrogen to keep the YBCO below the critical temperature of 86 K.

Fig. 6 shows the typical transmission characteristics of the YBCO-YIG composite structure MSSW waveguide for a zero air gap and for $H_0 = 130$ Oe. The dc magnetic field intensity of 130 Oe is inadequate to completely saturate the magnetization of the YIG film and as a consequence which will lead to increase the loss. The strong magnetic

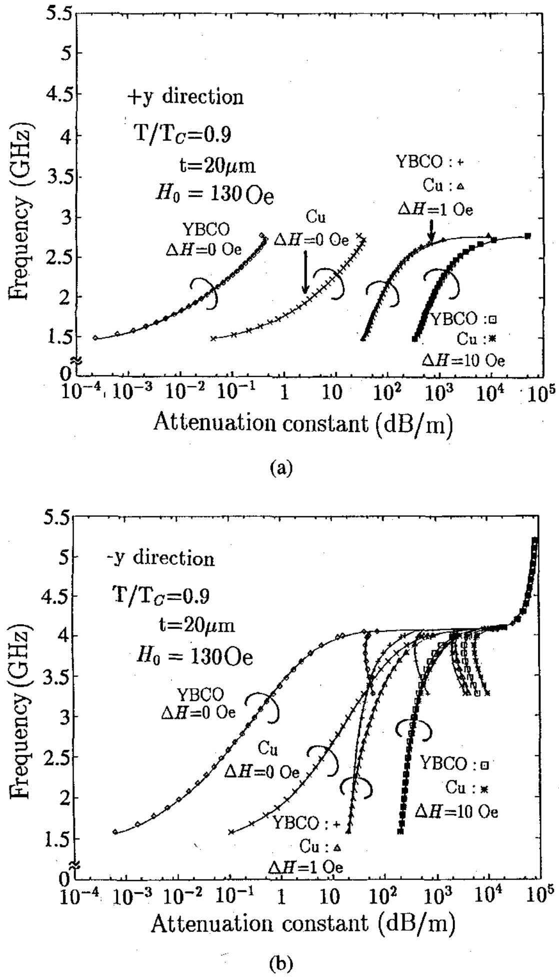

Fig. 4. Attenuation constant of the dispersion curve for an air gap of 20 μm.

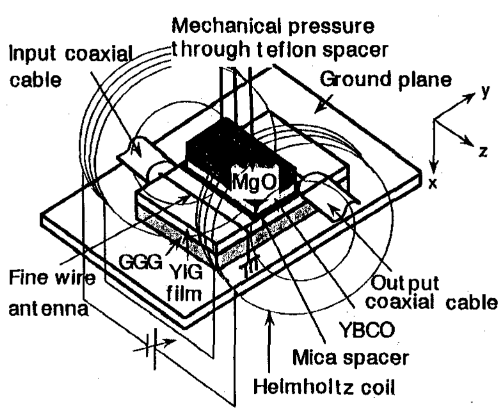

Fig. 5. Experimental set up.

field with high current was difficult to generate because of the limited heat capacity of the refrigerator. For comparison, Fig. 7 shows the characteristics of the copper-YIG composite structure for a zero air gap. Transmitted power S_{12} in the figures is observed by reversing the input and output ports or reversing the magnetic field direction. In Fig. 6 S_{12} is found to be weaker than S_{21} by 15 dB. Such a nonreciprocal behavior due to difference between S_{12} and S_{21} occurs for the asymmetric structure of the transducer, but it is small [10].

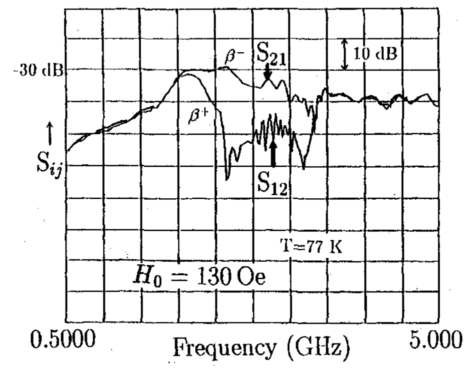

Fig. 6. Nonreciprocal transmission characteristics of the MSSW in the YBCO-YIG composite guide for a zero air gap.

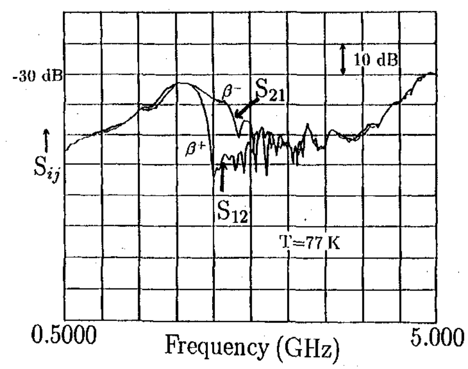

Fig. 7. Nonreciprocal transmission characteristics of the MSSW in the Cu-YIG composite guide for a zero air gap.

Thus, the nonreciprocal behavior of 15 dB can be seen in the frequency region from 2.45 GHz to 3.55 GHz. In contrast, the nonreciprocal behavior of the transmission characteristics of the copper-loaded waveguide of Fig. 7 is weaker and has a narrower bandwidth (0.5 GHz) than the YBCO-loaded waveguide of Fig. 6.

The enhancement of nonreciprocal characteristics by superconductivity was thus confirmed experimentally as discussed in Fig. 3.

The effect of the air gap on transmission characteristics was examined. Fig. 8 shows the transmission characteristics of a YBCO-YIG waveguide for a 20 μm air gap. For comparison, Fig. 9 shows the transmission characteristics of a copper-YIG waveguide for a 20 μm air gap. The bandwidths which exhibit nonreciprocity are reduced about 45% compared to the case of a zero air gap of Fig. 6. The effects of the air gap on the waveguide characteristics were thus confirmed by experiments to produce a narrow bandwidth (0.5 GHz) as discussed in Fig. 4. Through these experiments the insertion loss in the waveguide (30 dB) was relatively high. This may be attributed to the unsaturated magnetization for a low dc magnetic field with low electric current discussed above, and the large mismatch of impedance between the transducer and rf source. The latter could be confirmed by measuring scattering parameter of S_{11} for a high dc magnetic field, and the mismatch loss of 16 dB was evaluated including 6 dB on perfect matching condition. Group delay characteristics were

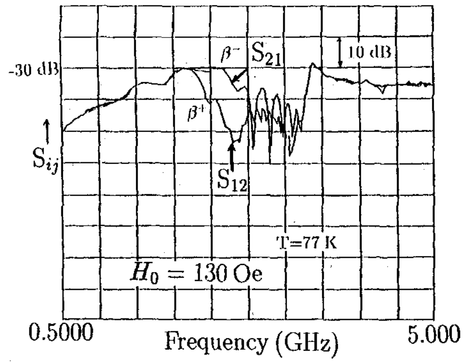

Fig. 8. Nonreciprocal transmission characteristics of the MSSW in the YBCO-YIG composite guide for a 20 μm air gap.

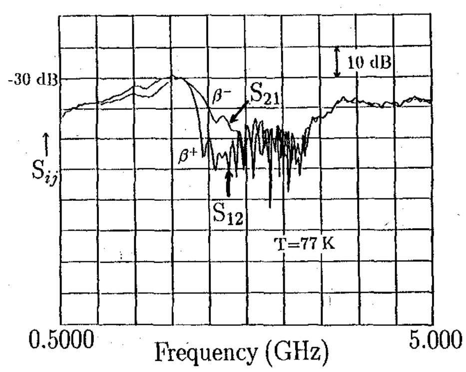

Fig. 9. Nonreciprocal transmission characteristics of the MSSW in the Cu-YIG composite guide for a 20 μm air gap.

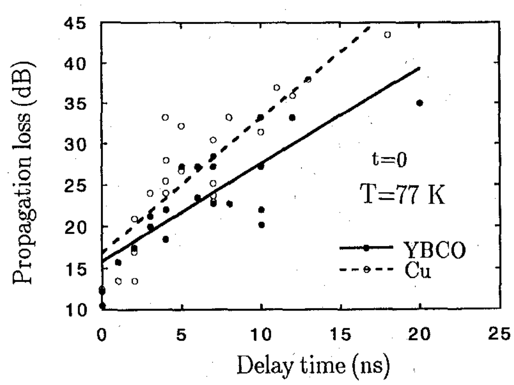

Fig. 10. Propagation loss characteristics versus group delay time at liquid nitrogen temperature.

also measured as a function of frequency from 2.5 GHz to 3.5 GHz both for copper and YBCO at 77 K for a zero air gap using a pulse technique. Fig. 10 shows the observed propagation loss versus group delay time for a pulsewidth of 100 nsec. It can be seen from Fig. 10 that loss was not significantly reduced due to the superconductor, and that there was only a few dB propagation loss difference between Cu and YBCO.

One reason why significant loss reduction was not observed may be due to increase more than 1 Oe in magnetic loss ΔH below the liquid nitrogen temperature due to rare earth impurities [11], [12]. To get significant loss reduction as predicted, the ΔH value should be around 0.2 Oe at liquid nitrogen temperature. Another reason may be the effect of relaxation of the GGG at 77 K due to the paramagnetic Gd ion.

IV. Conclusion

We have analyzed the propagation characteristics of MSSW in the YBCO-YIG multilayered structure. The effect of the superconductor on a MSSW waveguide has been examined from the dispersion characteristics of both the phase and attenuation constant as a function of the air gap between YIG and YBCO, taking into consideration the magnetic linewidth of the YIG film. Comparing calculations to experimental data, we found that the experimental bandwidth for allowing nonreciprocity can be varied by changing the air gap, and increases with superconductivity. However, we could not observe experimentally the strong nonreciprocity due to superconductivity that is predicted theoretically. This means that magnetic losses in the YIG and GGG samples used for the experiment were relatively large and may have increased at low temperature. To prevent these magnetic losses, it is necessary that single crystal slab of pure YIG ($\Delta H \simeq 0.2$ Oe) is used and YBCO is directly deposited on the YIG crystal [13]. The waveguide configuration proposed may have considerable potential as a nonreciprocal microwave circuit integrated with a superconductor [14].

Acknowledgment

The authors would like to thank to Dr. T. Inui and Dr. T. Yoshitake of the NEC Corporation for providing YBCO samples.

References

[1] Special Issue on Microwave Applications of Superconductivity, *IEEE Trans. Microwave Theory Tech.*, vol. 39, no. 9, Sept. 1991.

[2] E. Denlinger, R. Paglione, D. Kalokitis, E. Belohoubek, A. Pique, X. D. Wu, T. Venkatesan, A. Fathy, V. Pendrick, S. Green, and S. Maiheuss, "Superconducting nonreciprocal devices for microwave systems," *IEEE Microwave Guided Wave Lett.*, vol. 2, no. 11, pp. 449–451, Nov. 1992.

[3] G. F. Dionne, D. E. Oates, and D. H. Temme, "Low-loss microwave ferrite phase shifters with superconducting circuits," in *IEEE MTT-Symp. Dig.*, Jun. 1994, pp. 101–103.

[4] M. S. Pambianchi, D. H. Wu, L. Ganapathi, and S. M. Anlage, "DC magnetic field dependence of the surface impedance in superconducting parallel plate transmission line resonators," *IEEE Trans. Appl. Superconduct.*, vol. 3, no. 1, pp. 2774–2777, Mar. 1993.

[5] Special Section on Microwave Magnetics, *Proc. IEEE*, vol. 76, no. 2, Feb. 1988.

[6] W. L. Bongianni,"Magnetostatic propagation in a dielectric layered structure," *J. Appl. Phys.* vol. 43, no. 6, pp. 2541-2548, Jun. 1972.

[7] C. Vittoria and N. D. Wilsey, "Magnetostatic wave propagation losses in an anisotropic insulator," *J. Appl. Phys.* vol. 45, no. 1, pp. 414–420, Jan. 1974.

[8] K. K. Mei and G. C. Liang, "Electromagnetics of superconductors," *IEEE Trans. Microwave Theory Tech.*, vol. 39, no. 9, pp. 1545–1552, Sept. 1991.

[9] S. Miura, T. Yoshitake, H. Tsuge, and T. Inui, "Properties of shielded microstrip line resonators made from double-sided $Y_1Ba_2Cu_3O_x$ films," *J. Appl. Phys.* vol. 76, no. 7, pp. 4440–4442, Oct. 1, 1994.

[10] T. Omori, K. Yashiro, and S. Ohkawa, "A study on magnetostatic surface wave excitation by microstrip," *IEICE Trans. Electronics*, vol. E77-c, no. 2, pp. 312–318, Feb. 1994.

[11] C. Kittel, "Microwave resonance in rare earth iron garnets," *J. Appl. Phys. Sup.* vol. 31, no. 5, pp. 11S–13S, May 1960.

[12] J. F. Dillon, Jr. and J. W. Nielsen, "Ferrimagnetic resonance in impurity doped Yttrium Iron Garnet (YIG)," *J. Appl. Phys. Sup.* vol. 31, no. 5, pp. 43S–44S, May 1960.

[13] A. Pique, K. S. Harshavardhan, J. Moses, M. Matheer, E. Belohoubek, T. Venkatesan, E. J. Denlinger, D. Kalokitis, A. Fathy, V. Pendrick, M. Rajeswari, and Wu Jiang, "Microwave compatible $YBa_2Cu_3O_{7-x}$ films on ferrimagnetic garnet substrates," *Appl. Phys. Lett.* vol. 67, no. 12, pp. 1778–1780, Sept. 18, 1995.
[14] El-Badawy, El-Sharawy, and J. S. Guo, "Thin film isolators utilizing MSSW transducers," in *IEEE '95 MTT-Symp. Dig.*, TU1E-4, pp. 107–110, May 1995.

Makoto Tsutsumi (M'71) was born in Tokyo, Japan, on February 25, 1937. He received the B.S. degree in electrical enginerring from Ritsumeikan University, Kyoto, Japan, in 1961 and the M.S. and Ph.D. degrees in communication engineering from Osaka University, Osaka, Japan, in 1963 and 1971, respectively.

From 1984 to 1987 he was an Associate Professor of Commucation Engineering at Osaka University, Since 1988 he has been a Professor at Kyoto Institute of Technology, Department of Electronics and Information Science, Kyoto, Japan. His research interests are primarily in microwave and millimeter-wave ferrite devices and optics/microwave interactions in the semiconductor.

Takeshi Fukusako (S'94) was born in Miyazaki, Japan, on June 14, 1967. He received the B.E. and M.E. degrees in electronics and information science from Kyoto Institute of Technology, Kyoto, Japan, in 1992 and 1994, respectively. He is currently working toward the Ph.D. degree in the Department of Electronics and Information Science at Kyoto institute of Technology.

His reseach interests are high-temperature superconductor applications to microwave ferrite cicuits and devices.

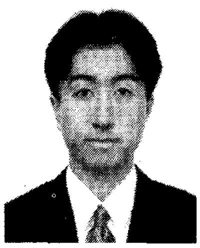

Shigeo Yoshida was born in Osaka, Japan, on July 7, 1972. He received the B.E. degree in electronics and information science from Kyoto Institute of Technology, Kyoto, Japan, in 1995. Currently, he is studying toward the M.E. degree in electronics and information science at the same institute.

His current interests are applications of high-T_c superconductors to microwave circuits.